

Article

Coating of Neural Electrodes with Platinum Nanoparticles Reduces and Stabilizes Impedance In Vitro and In Vivo in a Rat Model

Svilen D. Angelov¹, Christoph Rehbock², Vijayanthi Ramesh², Hans E. Heissler¹, Mesbah Alam¹ ,
Stephan Barcikowski² , Kerstin Schwabe¹ and Joachim K. Krauss^{1,*} 

¹ Department of Neurosurgery, Hannover Medical School, Carl-Neuberg-Str. 1, 30625 Hannover, Germany; svidel@protonmail.com (S.D.A.); boiteaulette@mac.com (H.E.H.); alam.mesbah@mh-hannover.de (M.A.); schwabe.kerstin@mh-hannover.de (K.S.)

² Technical Chemistry I and Center for Nanointegration Duisburg-Essen (CENIDE), University of Duisburg-Essen, Universitaetsstrasse 7, 45141 Essen, Germany; christoph.rehbock@uni-due.de (C.R.); vijayanthi.ramesh93@gmail.com (V.R.); stephan.barcikowski@uni-due.de (S.B.)

* Correspondence: krauss.joachim@mh-hannover.de; Tel.: +49-511-532-6651

Abstract: The efficacy of electrodes that are chronically implanted and used in the context of deep brain stimulation (DBS) for the treatment of neurological disorders critically depends on stable impedance. Platinum–iridium electrodes were coated with laser-generated platinum nanoparticle colloids (PtNPs) via electrophoretic deposition using pulsed direct currents (DC-EPD). Uncoated electrodes were used as controls. In vitro, electrodes were stimulated for four weeks in a 0.9% NaCl solution. For the in vivo (rats) study, coated electrodes were implanted in the left and uncoated control electrodes in the right subthalamic nucleus (STN). After two weeks of recovery, electrodes were stimulated for four weeks. Impedance measurements were conducted after each week of stimulation, both in vivo and in vitro. NP-coating resulted in a significant and long-lasting reduction in electrode impedance ($p < 0.05$) over four weeks of in vitro stimulation. Despite an initial increase in impedance after intracranial implantation, the impedance of the NP-coated electrodes was also reduced during in vivo stimulation over four weeks. NP-coated electrodes had a lower fluctuation of impedance during stimulation compared to uncoated electrodes both in vitro and in vivo ($p < 0.05$). Laser-generated PtNPs applied to electrodes by pulsed DC-EPD lead to lower and more stable electrode impedance during chronic stimulation, with the potential to enhance the performance of DBS systems during chronic use.

Keywords: nanoparticles; electrophoretic deposition; deep brain stimulation



Citation: Angelov, S.D.; Rehbock, C.; Ramesh, V.; Heissler, H.E.; Alam, M.; Barcikowski, S.; Schwabe, K.; Krauss, J.K. Coating of Neural Electrodes with Platinum Nanoparticles Reduces and Stabilizes Impedance In Vitro and In Vivo in a Rat Model. *Coatings* **2024**, *14*, 352. <https://doi.org/10.3390/coatings14030352>

Academic Editors: Valentina Grumezescu and Gabriela Dorcioman

Received: 25 January 2024

Revised: 5 March 2024

Accepted: 11 March 2024

Published: 15 March 2024



Copyright: © 2024 by the authors. Licensee MDPI, Basel, Switzerland. This article is an open access article distributed under the terms and conditions of the Creative Commons Attribution (CC BY) license (<https://creativecommons.org/licenses/by/4.0/>).

1. Introduction

Neural electrodes are implanted in the brain for the recording of neuronal activity and for electrical stimulation both in acute and chronic settings [1]. In particular, deep brain stimulation (DBS), with the option of closed-loop adaptive stimulation, has gained widespread attention [2,3]. The efficacy of the electrodes depends on the material's properties, which account for the stabilization of the electrode impedance, directly affecting electrical stimulation or recording. Approaches in this context are nanoscopic structuring via chemical surface modification techniques [4], laser-based patterning techniques [5], or deposition of nanoscale materials on the electrode surface by either the sputtering of iridium oxide [6] or chemical reduction methods (platinum grass) [7–9]. These techniques reduce electrode impedance [7,10], although sufficient in vivo performance remains to be shown for long-term applications.

Electrophoretic deposition (EPD) is another well-established coating method for solids based on the movement of charged colloidal particles in an electric field towards an oppositely-charged counter electrode, followed by the controlled deposition of the particles on the surface. As well as industrial and energy applications, EPD is used to generate

biomaterials including neuro-electrodes [11]. In contrast to other modification methods, however, the EPD of laser-generated platinum (Pt) nanoparticles (Pt-NP) on the surface of platinum–iridium (Pt–Ir) electrodes increases their impedance in vitro [12]. After intracranial implantation in a rat model, impedance was further enhanced, temporarily. Nevertheless, during stimulation over three weeks, the electrodes that were coated with Pt-NP of less than 10 nm had the most stable impedance dynamics, while the impedance of the uncoated electrodes continued to increase over time [12].

Unlike DC-EPD, during processing with pulsed DC-EPD, the field is turned off 50% of the time, which counteracts the electro-osmotic and electrohydrodynamic forces and avoids the formation of assemblages [13]. Indeed, pulsed DC-EPD yields homogeneous coatings on Pt–Ir electrodes, while large assemblages dominate DC-EPD-coated samples. Moreover, pulsed DC coatings reduce impedance in comparison to uncoated and DC EPD-coated electrodes [14]. So far, the mechanical stability of pulsed DC-EPD coatings has been verified in vitro and in vivo, thus supporting the clinical applicability of the designed coatings [15]. Furthermore, Cyclic Voltammetry has been used to assess the electrochemical properties of electrodes and to characterize electrodes before determining the electro-catalytic surface area; pronounced changes due to the surface coverage [16], using EPD in pulse mode (DC vs. pulsed DC), and the solvent used were found [14].

Here, we examined whether the impedance of neural electrodes coated via pulsed DC-EPD would change after intracranial implantation in rats, followed by four weeks of in vivo stimulation. We also performed a four-week in vitro stimulation of NP-coated and uncoated electrodes in saline solution. From a fundamental viewpoint, these experiments will help to clarify how the impedance of electrodes changes in vivo based on the initially applied coating properties. Furthermore, these experiments may help to elucidate to what extent changes in impedance during long-term in vivo trials depend on the properties of the electrode, interactions with brain tissue, the stimulation applied, or a combination thereof.

2. Materials and Methods

2.1. Nanoparticle Synthesis

The Pt nanoparticles used for the EPD coating process were fabricated by laser processing in liquids using a two-step procedure, including a process termed laser ablation in liquids (LAL) of a platinum target in water, yielding a polydisperse Pt colloid, and subsequent laser fragmentation in liquids (LFL) in a liquid jet reactor, which leads to efficient particle size reduction and a narrowing of the particle size distribution. Details on the synthesis process and further colloid characterization can be found in our previous work [14].

2.2. Electrodes and Coating

Two parallel Pt–Ir (90:10) wires that were insulated with PTFE ($d = 0.0055$ with insulation and $d = 0.003$ uninsulated; Science-Products GmbH, Hofheim, Germany) were placed in a stainless steel tube (0.55×17 mm) that was cut from a 24 G syringe needle (for more details, see [12]). At the contact end, the isolation was removed with scalpel blades under a stereomicroscope-Zeiss (Carl Zeiss Microscopy GmbH, 07745 Jena, Germany), leaving a 500 μm -long bare surface with an approximately 250 μm intercontact distance. Contact pins were soldered to the other end. The electrode tip was cleaned and conditioned before coating by immersing it in 65% nitric acid for 15 min. After this, it was rinsed thoroughly with distilled water.

The NPs were deposited on the neural electrode contact surface via EPD using pulsed DC electric fields, a procedure described in our previous work in more detail [14]. In short, pulsed DC fields (50% duty cycle, 1 μs period) with a field strength of 5 V/cm and a deposition time of 10 min were applied. The deposition was carried out in an aqueous solution at alkaline pH. Two sets of pulsed-DC coated electrodes were used for the in vitro and the in vivo experiments. In total, 16 samples were coated for in vitro and in vivo stimulation experiments. As controls, another 16 electrodes were immersed in the Pt colloids for 10 min without applying an electric field.

2.3. Impedance Measurement

The impedance of the electrodes was determined by applying Ohm's law at a single frequency of 200 Hz, as described in [12,14]. After immersion in saline solution (0.9% NaCl), a sinusoidal voltage (200 mV p-p) was applied to the electrodes. Thereby, a current was driven through both an electrode and a serial-measurement resistor ($200 \pm 1\% \Omega$). This current is proportional to the voltage drop across the measurement resistor. After feeding the voltage into a precision differential amplifier (AMP01, Analog Devices, Inc., Norwood, MA, USA), the amplifier output voltage allowed for the calculation of the current amplitude. The electrode's resistance was then estimated by applying Ohm's law. Thereafter, we verified the capacitive reactance by phase shifting of the test voltage and current (for more detail, see [12,14]). The above-described methodology was used for both in vitro and in vivo impedance measurements.

Notably, the first impedance measurement was performed after cleaning in 65% nitric acid for 15 min before coating to exclude changes induced by the cleaning procedure.

2.4. Animals

For the in vivo study, male Sprague Dawley rats ($n = 8$) were obtained from Charles River Laboratories, Germany, as done before for other work carried out by our group [12,14]. In our facility, groups of rats ($n = 2-4$) were kept in Macrolon Type IV cages (Techniplast, Hohenpeissenberg, Germany) in a climatized room. The temperature was kept at 22°C with the light on for 14 h and lights off for 10 h, with lights on at 07:00 a.m. Following the surgical procedure, each rat was kept in a standard Macrolon Type III cage. The rats were provided with laboratory rat chow and tap water.

The experimental protocols used in this study followed national and international ethical guidelines (see German Animal Welfare Act). Experiments started after approval by the local authorities (AZ 18/2837), including an animal ethics committee approval. This study was performed in accordance with the Animal Experiments Act guideline: Reporting of In Vivo Experiments (ARRIVE).

2.5. Surgery

For surgery, we used the procedure described before by our group [12,14]. After intraperitoneal injection of chloral hydrate (360 mg/kg) for anaesthesia, rats were placed into a stereotaxic frame. Additionally, a local anaesthetic (2% prilocaine hydrochloride) was introduced into the surgical site. Following the initial incision and identification of the bregma point, a pair of burr holes were created on both sides directly above the desired targets. The electrodes were bilaterally implanted in the subthalamic nucleus (STN) of the rats ($n = 8$) with coated electrodes implanted in the left hemisphere and uncoated electrodes in the right hemisphere as an internal control. Using the bregma point for reference, electrodes were implanted -3.8 mm, mediolateral: $+/-2.5$ mm, dorsoventral: -8.0 mm. Additionally, the tooth bar was adjusted to a position of -3.3 mm. Thereafter, we fixed the implanted electrodes with dental acrylic cement (Paladur[®], Heraeus Kulzer GmbH, Hanau, Germany) using screws (1×2 mm) as reinforcement in the skull bone. Starting preoperatively (two days), rats received a subcutaneous injection of marbofloxacin, 6.6 mg/kg, as an antibiotic for eight days. The analgetic carprofen (5 mg/kg) was subcutaneously injected intraoperatively and for the first two postoperative days (Figure 1).

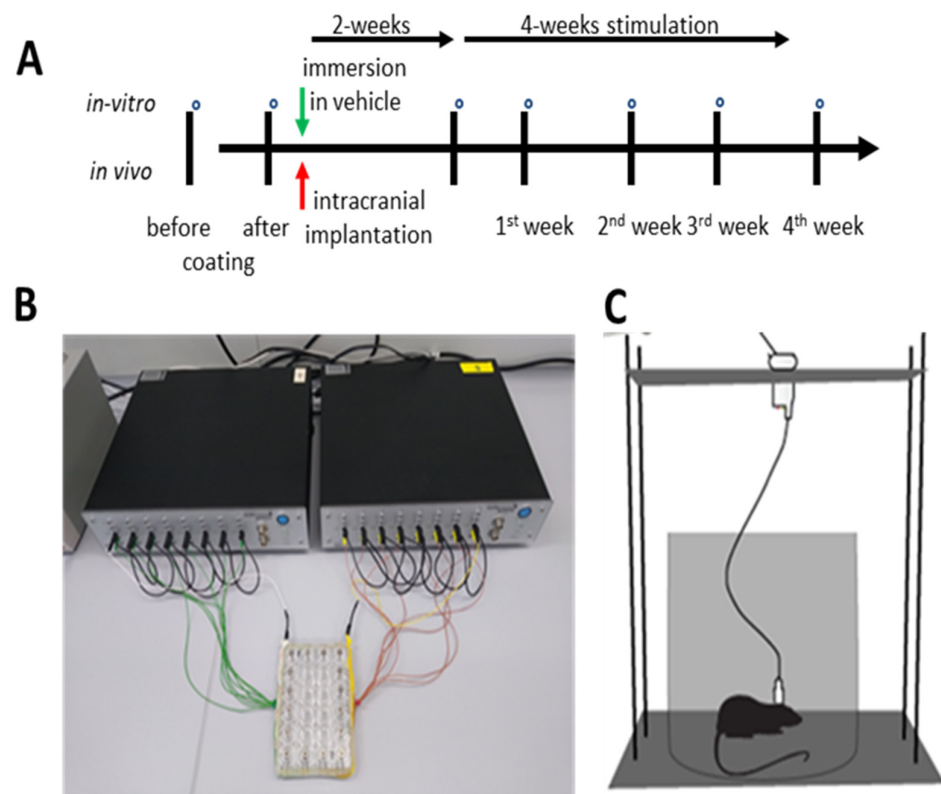


Figure 1. Schematic drawing for the in vitro/in vivo experiments with impedance measurements depicted as ° (A). In a stimulation, the chamber electrodes were immersed in saline solution (0.9% NaCl) for in vitro measures (B). For in vivo measures, the rat's head stage was connected to the stimulation device and impedance was measured in the awake, free-moving rat once a week (C).

2.6. Electrostimulation

In vivo: After two weeks of postoperative recovery, the animals received chronic stimulation for four weeks. Each rat was single housed in a standard Macrolon Type III cage during continuous stimulation. A slot in the lid allowed free movement of the animal with the cable attached. The cable was protected against biting by a spring-like metal shield and connected the skull socket and the stimulation device (Multichannel Systems STG2008, Software: Mc-Stimulus II). A swivel (Plastics one Inc., Roanoke, VA, USA) in between allowed the rat to move freely. Electrical stimulation was delivered using symmetric, bipolar, rectangular waves with a pulse width of 160 μs and a frequency of 130 Hz. The amplitude of the pulse was determined to be 20% below the individual motor response level, as described in our previous setting [13], which was on average 156 ± 17.9 (S.E.M) μA , which is within the typical range for STN-DBS in rodents [17]. We controlled the stimulation parameters with an oscilloscope (Tektronix TDS2000C, Beaverton, OR, USA), as described in the authors' previous work [15]. Thereafter, the impedance was measured weekly until the 4th week of stimulation, but there was no need for further adjustment.

In vitro: coated and uncoated control electrodes ($n = 8$ each) were immersed in 0.9% NaCl solution, in separate wells of a standard 24-well cell culture plate with a modified lid with openings, fixators, and contacts for the electrodes (Figure 1). The electrodes were left unplugged for two weeks (to simulate the in vivo postoperative period); after this, continuous electrostimulation with a pulse amplitude of 200 μA was conducted for four weeks.

2.7. Histology

After the end of the experiments, the implantation sites were histologically verified by referring to the rat brain atlas [18]. An overdose of chloral hydrate was injected and, after reaching deep anaesthesia, rats were perfused transcranially with 4% paraformaldehyde

solution. Thereafter, we removed the brain from the skull and immersed them for at least 12 h in 30% sucrose/phosphate-buffered saline (PBS). With the help of a freezing microtome, coronal planes (width of 40 μm) were cut and, after Nissl staining with Thionin, used to validate the correct position of the electrodes under a light microscope (Zeiss, Göttingen, Germany).

2.8. Statistical Analysis

For statistical evaluation of the impedance dynamics *in vitro* and *in vivo*, data was analysed by non-parametric one-way ANOVA (Friedman), followed by a post-hoc Dunn's test. In addition, the measures of all groups were compared after calculating the relative impedance to the preoperative measures, which were set at 100%. Thereafter, groups were compared by using a Kruskal–Wallis ANOVA followed by a post-hoc Dunn's test after coating, post-OP, and during stimulation (1st to 4th week). All tests were performed two-sided, with $p < 0.05$ considered statistically significant.

3. Results

3.1. Characterization of Nanoparticles and Electrode Coatings

A representative UV-Vis spectrum of the colloidal Pt nanoparticles shows Pt's typical broadband extinction behaviour, with a peak at 260 nm (Figure 2A) attributed to the presence of Pt–water complexes [19], indicating the partial oxidation of the generated nanoparticles. Oxidation of Pt nanoparticles is commonly reported in the laser synthesis of nanoparticles in liquids [20], which is the main reason for the negative surface charge (zeta potential) of the Pt colloids (data not shown here, but reported in previous works [16,21]). The particle size distributions of the colloidal Pt nanoparticles analysed by analytical disk centrifugation exhibited monodispersity, with a median diameter of ~ 10 nm (Figure 2B)—the particle size that proved to be most efficient concerning the impedance stabilization of neural electrodes *in vivo* in our previous work [12].

The deposited mass of Pt was determined via an analysis of the UV-Vis spectra before and after the coating process (Figure 2C). Here, a reduction in absorbance was observable over the whole spectral range after coating, which indicated a loss of platinum mass in the colloid, indicating deposition on the electrodes. The utilization of UV-Vis spectroscopy to evaluate mass loss in the supernatants, associated with particle deposition, has been established in our previous works [14,22]. Quantification of the deposited mass was conducted using a calibration curve, in which the area under the curve of the UV-Vis spectra in a spectral range of 190–900 nm was plotted against the known mass concentrations of the reference Pt colloids (Figure S1). The total deposited mass of Pt nanoparticles on the electrodes (mean and standard deviation of 16 samples) was 3.4 ± 0.8 μg . The coatings of the electrodes were further characterized by SEM analysis (Figure 1C). Here, homogeneous coatings were formed on the EPD-coated electrodes, with results similar to those reported previously upon utilization of pulsed DC-EPD [14]. The immersed samples showed minute particle deposition, with very few particles sticking to the electrode surface. This finding indicated that the coating is formed due to the application of the electric field and not solely by adsorption from the solution. As expected, the control sample (not in contact with the Pt colloid) showed a smooth surface without nanoparticles.

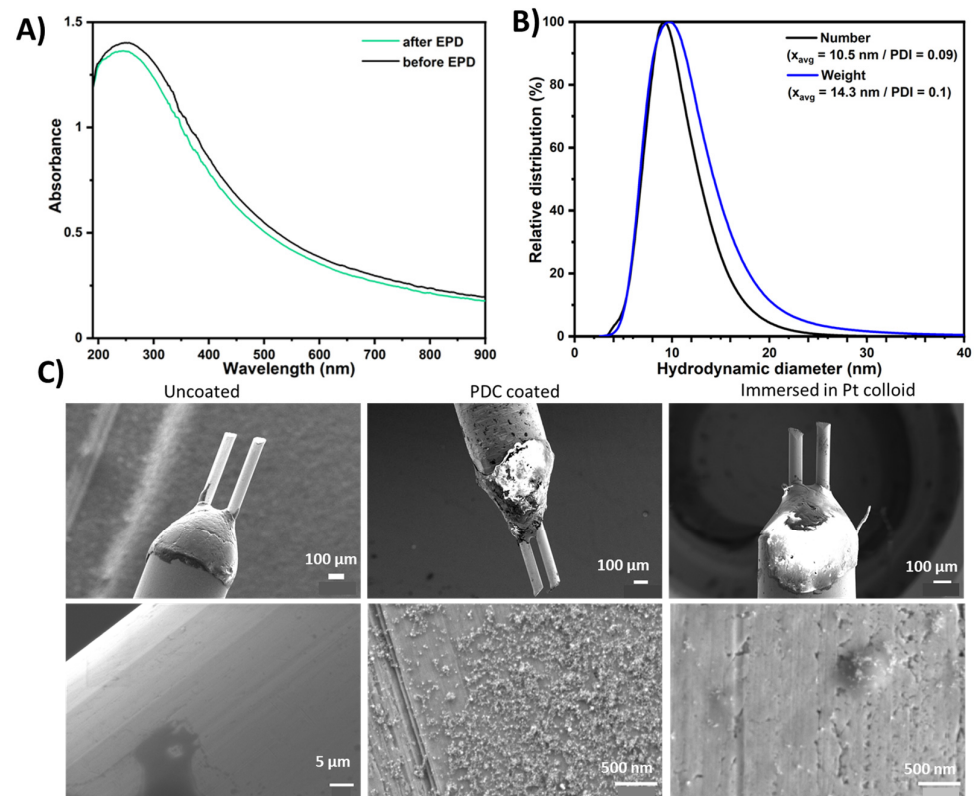
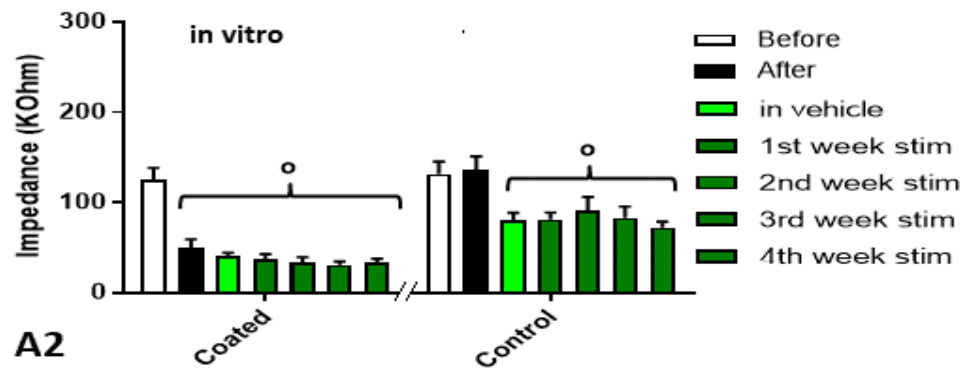


Figure 2. Characterization of colloidal nanoparticles and coated electrodes: (A) Representative UV-Vis extinction spectra of Pt nanoparticle colloids before and after EPD coating. (B) Representative hydrodynamic particle size distribution of platinum nanoparticle colloid, determined by analytical disk centrifugation. Mean values were determined from the median values of a log-normal fit of the corresponding distributions, PDI = Polydispersity index. (C) Representative SEM images (overview top row and higher magnification bottom row) of uncoated (left), pulsed DC-coated (middle), and immersed (right) neural electrodes. The electrodes consisted of two Pt metal tips, which were coated by EPD.

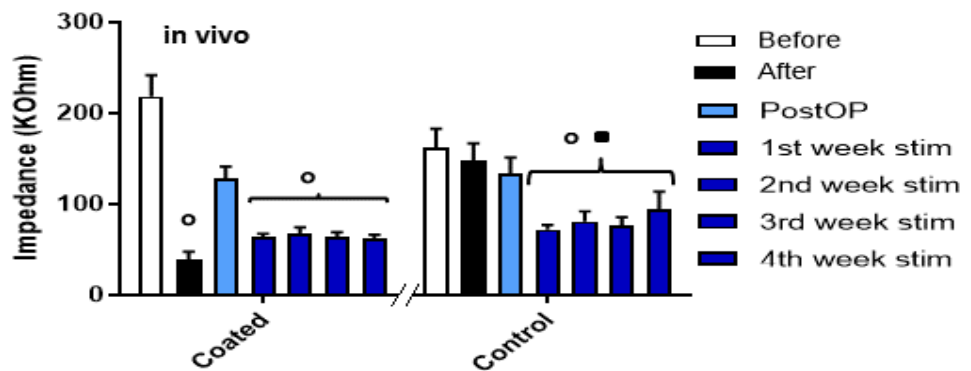
3.2. Impedance In Vitro

For the coated group, eight electrodes were analysed and eight electrodes formed the control group. For the in vitro measurements, statistical analysis of the impedance of coated electrodes using a non-parametric one-way ANOVA (Friedman) revealed a significant effect in both the coated (Chi-Square = 24.85, $df = 6$, $p < 0.001$) and uncoated electrodes (Chi-Square = 28.54, $df = 6$, $p < 0.001$). Post-hoc testing revealed that NP-coating significantly reduced impedance ($p < 0.001$), while dipping of the control electrodes into the NP-colloid did not affect impedance. Immersion of the coated electrodes into the saline solution had no effect; however, in control electrodes, the impedance was reduced upon immersion in saline ($p < 0.05$). During stimulation for four weeks, the impedance of the coated electrodes in vitro was stable, whereas in the control samples, the impedance varied to some extent (Figure 3A1).

A1



A2



B

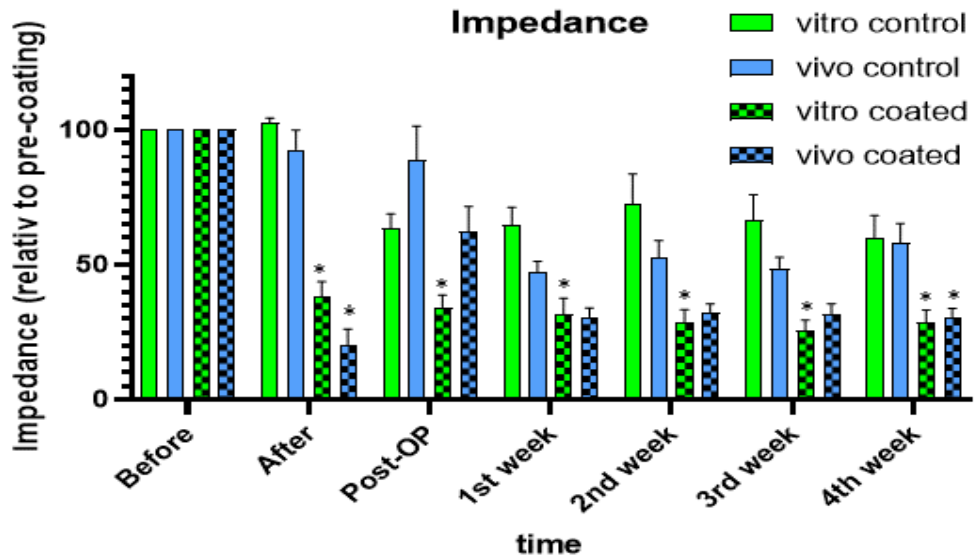


Figure 3. Impedance of electrodes: Impedance of electrodes after NP-coating or immersion into NP solution as a control and subsequent immersion into vehicle solution (A1) or intracranial implantation in rats (A2). Significant differences to “before” coating data are depicted as a circle (°), and to “after” coating data as a square (X; $p < 0.05$ after one-way ANOVA and post-hoc testing). Relative impedance of all groups for all times, with significant differences between uncoated and coated electrodes shown as asterisks (*; $p < 0.05$ after two way ANOVA and post-hoc testing (B)).

3.3. Impedance In Vivo

The histological analysis showed that all NP-coated and uncoated electrodes ($n = 8$, each) were placed in the STN of the left and right hemispheres. As one electrode of each

group broke during the experiments, seven electrodes were used for statistical analysis of the impedance measurements. Statistical analysis of the impedance of the coated and uncoated electrodes over time with one-way ANOVA (Friedman) showed a significant effect in both coated (Chi-Square = 30.92, $df = 6$, $p < 0.001$) and uncoated electrodes (Chi-Square = 31.28, $df = 6$, $p < 0.001$). Post-hoc testing revealed that NP-coating significantly reduced impedance ($p < 0.001$) before implantation and over four weeks of stimulation (all $p < 0.05$), whereas impedance two weeks after implantation was temporarily enhanced. Dipping of electrodes in NP solution and intracranial implantation did not affect impedance. In contrast, during the first three weeks of stimulation, the impedance of the uncoated electrodes was significantly reduced, compared to the impedance before and after dipping in NP-solution (all $p < 0.05$; Figure 3A2).

3.4. Normalized Data

For better comparability between the groups and to cancel out impedance differences between individual groups of electrodes, all data was normalized by the impedance of the corresponding uncoated electrodes (white bars in Figure 3A1,A2 set as 100%). Thereafter, groups were compared using a Kruskal–Wallis ANOVA followed by a post-hoc Dunn’s test after coating, post-OP, and during stimulation (1st to 4th week). Post-hoc comparison after a significant Kruskal–Wallis with Dunn’s test showed that NP-coating significantly reduced impedance in electrodes assigned to both in vitro and in vivo groups ($p < 0.05$). As after intracranial implantation, the impedance of NP-coated electrodes was increased (see Figure 3A2), the difference between coated and uncoated electrodes was temporarily lost. During the four weeks of stimulation, the impedance of the coated electrodes was reduced compared to the uncoated electrodes for both the in vivo and in vitro approaches, although after intracranial implantation, this effect only reached the level of significance on the 4th week following implantation ($p < 0.05$; $p < 0.1$; Figure 3B).

In addition, we applied Levene’s test to assess whether the coated and uncoated electrodes’ impedance would differ in their variance. According to Levene, comparative statistics of the dispersion of pooled impedance values of coated and uncoated control electrodes under stimulation in vitro and in vivo showed that the variances over the four weeks of stimulation were not equal. Likewise, Bartlett’s test of homogeneity of variances showed that the variances of the electrode impedances differed over four weeks of stimulation (see Table 1).

Table 1. Statistics for the dispersion of pooled impedance values of coated and uncoated control electrodes under stimulation in vitro and in vivo (for description, see text).

	In Vitro	In Vivo
mean \pm SD, impedance in k Ω coated/uncoated (ctl)	33.8 \pm 12.7/82.0 \pm 29.9	64.8 \pm 13.2/81.3 \pm 31.9
LEVENE	F(1,58) = 12.126, $p = 0.001$	F(1,54) = 5.521, $p = 0.0225$
BARTELETT	$\chi^2 = 18.050$, $p < 0.0001$	$\chi^2 = 18.342$, $p < 0.0001$

4. Discussion

We showed that the pulsed DC-EPD of laser-generated PtNPs reduces and stabilizes impedance during long-term stimulation in saline, and after intracranial implantation into the rat brain with subsequent long-term stimulation.

In a previous study, we already demonstrated that NP-coating stabilizes the impedance of electrodes after intracranial implantation and long-term stimulation [12]. In that previous study, however, electrode impedance was increased after NP-coating via DC-EPD. In contrast, in the present study, pulsed DC-EPD was used for coating, based on our more recent work [14], which resulted in a reduced impedance. This finding is most likely attributed to the higher coating homogeneity achievable by pulsed DC-EPD, which also reduces impedance in an in vitro setting [14]. This reduced impedance in more homogeneous coatings was attributed to a higher active surface area, not driven by the geometric surface

area, but by an enhanced chemical activity and oxidation state of the surface atoms [16]. This was verified by XPS measurements of the coated electrodes, where about 40% of the Pt surface atoms were oxidized, whereas only up to 15% were oxidized in the uncoated sample. Furthermore, chemical activity was determined by cyclic voltammetry, and an elevated electrochemical surface area (ECSA) was found in the coated samples at a surface coverage with Pt nanoparticles of >10% [16].

In particular, the impedance of the NP-coated electrodes temporarily increased immediately after implantation in the rat brain. This observation corroborates our previous measures of elevated impedance after implantation into the rat brain [12], a finding also reported by other groups [23–25]. This finding is most likely attributed to the acute neural tissue response around the electrode [26–30] and appears as a spike in the impedance measurement [25,27]. This acute postoperative tissue reaction is followed by a chronic one—in particular, a moderate gliosis [25,31], which roughly corresponds to the reduced impedance measurement at the start of our electrostimulation period two weeks after intracranial implantation. Noteworthy, in a previous work, we examined the EPD coatings after a four week stimulation period by SEM, and we found that the coating was mostly intact, which seems to indicate that delamination of the coating is minimal—even under *in vivo* stimulation conditions [15]. Furthermore, previous work *in vivo*, we showed that NP-coating does not affect glial reactions or the number of neural cells in the vicinity of the electrode tip, and there were no significant differences in the statistical analysis of densitometric data from astroglial responses around electrode tips between groups using NP-coated and non-NP-coated electrodes [12]. Our parallel *in vitro* measurements in saline did not show enhanced impedance, confirming our hypothesis that an acute postoperative tissue reaction leads to enhanced electrode impedance in the *in vivo* setting. Interestingly, immersion of uncoated electrodes into saline reduced impedance, which is likely due to differences in the chemical composition of the different environments [32]. In addition, the average temperature of the *in vitro* lab solution was 23 °C (room temperature), while the temperature *in vivo* (in living organisms) ranges from 36 °C to 38.8 °C. Thus, the temperature differences between *in vivo* and *in vitro* settings may have influenced our results.

Increased impedance values of electrodes after intracranial implantation were statistically not different in coated and uncoated electrodes. We showed that glial reactions and neuronal loss do not differ between NP-coated and uncoated electrodes [12]. With the onset of stimulation, however, impedance decreased in NP-coated and uncoated electrodes, possibly due to intrinsic changes in the electrode. A similar phenomenon was observed when we cycled the coatings multiple times in an electrochemical cell [15]. As changes in impedance occur in parallel in *in vivo* and *in vitro* stimulated electrodes, it is plausible that the intrinsic effects of the electrodes are primarily responsible.

In general, an increase in impedance over time is expected due to tissue deposition or microglial interactions. However, continuous stimulation may prevent the buildup of tissue and protein on the electrode surface, maintaining better electrical contact and signaling, and reducing impedance. In fact, clinical studies in PD patients have shown that impedance gradually decreases over time, even when DBS settings are kept constant [33,34]. Nonetheless, although the impedance of coated electrodes is reduced during four weeks of stimulation as compared to uncoated control electrodes, there is no difference in the impedance between *in vivo* and *in vitro* settings, indicating that tissue reactions and scar formation seem to have no pronounced effect on stimulation efficiency in a chronic setting.

In the clinical context, NPs derived by laser ablation in liquid followed by electrophoretic deposition on electrodes of the same material allows for a homogenous coating without chemical precursors and ligands that may trigger a tissue response [35–38]. Although water–ethanol mixtures can lead to even more homogeneous coatings and more favorable electrochemical properties [39], we deliberately used samples from pulsed DC-EPD synthesis in water for the present experiments, as utilization of solvents should be avoided in experimental animal studies or clinical settings. Previous electron microscopic studies from our groups as well as other studies [14,40,41] have revealed that EPD offers good controllability and is suitable for depositing relatively thick coatings with moderate uniformity. Moreover, the mechanical

stability of the pulsed DC-EPD of PtNPs onto Pt-based neural electrodes has already been demonstrated using agarose gel, adhesive tape, and ultrasonication-based stress tests that simulate brain environments. In addition, it has been evidenced that NPs can still be found on an exemplarily explanted electrode surface after in vivo stimulation experiments [15].

However, a chronic response may affect stimulation outcome in ways that are not correlated with changes in impedance. Chronic DBS has been reported to affect neural network behavior or tissue responses to stimulation, altering stimulation efficacy even when impedance remains unchanged [42]. Impedance is expected to depend primarily on the diffusion geometry and diffusion length distribution in the nanoparticles. In addition, an improved electrode–electrolyte interface, a barrier layer effect, increased surface area, and the controlled size and geometry of the dispersed nanoparticles may collectively lead to a reduction in electrode impedance [8,43].

In conclusion, the pulsed DC-EPD of colloidal, ligand-free PtNPs on neural electrodes reduces impedance, favoring stimulation efficiency and possibly prolonging the battery life of the pulse generator. Studies and clinical applications for neuronal recording studies of EPD coatings show advantages, as it is applicable on a wide range of shapes with complex geometry and porous structures, uniform deposition, good control over layer thickness, and high homogeneity of the applied structure [44,45]. Additionally, as the coating and the implant material are identical, adverse effects concerning the biocompatibility of the electrode are unlikely, and thus clinical approval would be less complicated. From the viewpoint of medical applications, the pulsed DC-EPD of PtNPs may be a useful approach for generating an optimized nano-coating, which would reduce and restabilize the overall impedance in vivo and enhance the quality and durability of chronic recordings and stimulations in patients with electrical implants for therapeutic use over decades.

Supplementary Materials: The following supporting information can be downloaded at: <https://www.mdpi.com/article/10.3390/coatings14030352/s1>, Figure S1 showing a calibration curve used to correlate the UV-Vis AUC of spectra with the Pt mass concentration.

Author Contributions: S.D.A., K.S., C.R., S.B. and J.K.K. took part in the study concept and design. S.D.A. performed the in vivo experiments, histochemistry statistical analysis of the collected data and wrote the first draft of the manuscript. S.D.A., M.A. and H.E.H. did the impedance measurements. K.S. participated in the statistical analysis and manuscript drafting. C.R. and V.R. carried out the laser ablation and electrophoretic deposition of nanoparticles. K.S., C.R., S.B. and J.K.K. study supervision and coordination and also took part in the critical revision of the manuscript correction. All authors have read and agreed to the published version of the manuscript.

Funding: This work is supported by the German Research Foundation (DFG) grants KR 2931-3-1 and BA 3580-8-1.

Institutional Review Board Statement: All methods described were carried out in compliance with guidelines and regulations at the Hannover Medical School. All experimental protocols followed the German Animal Welfare Act, including approval of the Niedersaechsisches Landesamt fuer Verbraucherschutz und Lebensmittelsicherheit, Dezernat 33/Tierschutz; AZ 18/2837.

Informed Consent Statement: All co-authors have seen and agree with the contents of the manuscript and there are no financial interests to report.

Data Availability Statement: All data and material are presented in the main manuscript and additional supporting files are available from corresponding author on reasonable request.

Acknowledgments: The authors thank Jürgen Wittek for his expert technical assistance.

Conflicts of Interest: The authors declare that they have no conflicts of interest.

References

1. Schulder, M.; Mishra, A.; Mammis, A.; Horn, A.; Boutet, A.; Blomstedt, P.; Chabardes, S.; Flouty, O.; Lozano, A.M.; Neimat, J.S.; et al. Advances in Technical Aspects of Deep Brain Stimulation Surgery. *Stereotact. Funct. Neurosurg.* **2023**, *101*, 112–134. [[CrossRef](#)] [[PubMed](#)]
2. Krauss, J.K.; Lipsman, N.; Aziz, T.; Boutet, A.; Brown, P.; Chang, J.W.; Davidson, B.; Grill, W.M.; Hariz, M.I.; Horn, A.; et al. Technology of Deep Brain Stimulation: Current Status and Future Directions. *Nat. Rev. Neurol.* **2021**, *17*, 75–87. [[CrossRef](#)] [[PubMed](#)]

3. Lozano, A.M.; Lipsman, N.; Bergman, H.; Brown, P.; Chabardes, S.; Chang, J.W.; Matthews, K.; McIntyre, C.C.; Schlaepfer, T.E.; Schulder, M.; et al. Deep Brain Stimulation: Current Challenges and Future Directions. *Nat. Rev. Neurol.* **2019**, *15*, 148–160. [[CrossRef](#)] [[PubMed](#)]
4. Lord, M.S.; Foss, M.; Besenbacher, F. Influence of Nanoscale Surface Topography on Protein Adsorption and Cellular Response. *Nano Today* **2010**, *5*, 66–78. [[CrossRef](#)]
5. Kasemo, B. Biological Surface Science. *Surf. Sci.* **2002**, *500*, 656–677. [[CrossRef](#)]
6. Curtis, A.; Wilkinson, C. Nanotechniques and Approaches in Biotechnology. *Trends Biotechnol.* **2001**, *19*, 97–101. [[CrossRef](#)] [[PubMed](#)]
7. Boehler, C.; Stieglitz, T.; Asplund, M. Nanostructured Platinum Grass Enables Superior Impedance Reduction for Neural Microelectrodes. *Biomaterials* **2015**, *67*, 346–353. [[CrossRef](#)] [[PubMed](#)]
8. Boehler, C.; Vieira, D.M.; Egert, U.; Asplund, M. NanoPt-A Nanostructured Electrode Coating for Neural Recording and Microstimulation. *ACS Appl. Mater. Interfaces* **2020**, *12*, 14855–14865. [[CrossRef](#)]
9. Curtis, A.; Wilkinson, C. Topographical Control of Cells. *Biomaterials* **1997**, *18*, 1573–1583. [[CrossRef](#)]
10. Cassar, I.R.; Yu, C.; Sambangi, J.; Lee, C.D.; Whalen, J.J.; Petrossians, A.; Grill, W.M. Electrodeposited Platinum-Iridium Coating Improves In Vivo Recording Performance of Chronically Implanted Microelectrode Arrays. *Biomaterials* **2019**, *205*, 120–132. [[CrossRef](#)]
11. Fountas, K.N.; Smith, J.R.; Murro, A.M.; Politsky, J.; Park, Y.D.; Jenkins, P.D. Implantation of a Closed-Loop Stimulation in the Management of Medically Refractory Focal Epilepsy: A Technical Note. *Stereotact. Funct. Neurosurg.* **2005**, *83*, 153–158. [[CrossRef](#)] [[PubMed](#)]
12. Angelov, S.D.; Koenen, S.; Jakobi, J.; Heissler, H.E.; Alam, M.; Schwabe, K.; Barcikowski, S.; Krauss, J.K. Electrophoretic Deposition of Ligand-Free Platinum Nanoparticles on Neural Electrodes Affects Their Impedance in Vitro and in Vivo with No Negative Effect on Reactive Gliosis. *J. Nanobiotechnol.* **2016**, *14*, 3. [[CrossRef](#)]
13. Ristenpart, W.D.; Aksay, I.A.; Saville, D.A. Electrohydrodynamic Flow around a Colloidal Particle near an Electrode with an Oscillating Potential. *J. Fluid Mech.* **2007**, *575*, 83–109. [[CrossRef](#)]
14. Ramesh, V.; Rehbock, C.; Giera, B.; Karnes, J.J.; Forien, J.-B.; Angelov, S.D.; Schwabe, K.; Krauss, J.K.; Barcikowski, S. Comparing Direct and Pulsed-Direct Current Electrophoretic Deposition on Neural Electrodes: Deposition Mechanism and Functional Influence. *Langmuir* **2021**, *37*, 9724–9734. [[CrossRef](#)]
15. Ramesh, V.; Stratmann, N.; Schaufler, V.; Angelov, S.D.; Nordhorn, I.D.; Heissler, H.E.; Martínez-Hincapié, R.; Čolić, V.; Rehbock, C.; Schwabe, K.; et al. Mechanical Stability of Nano-Coatings on Clinically Applicable Electrodes, Generated by Electrophoretic Deposition. *Adv. Healthc. Mater.* **2022**, *11*, e2102637. [[CrossRef](#)]
16. Koenen, S.; Rehbock, C.; Heissler, H.E.; Angelov, S.D.; Schwabe, K.; Krauss, J.K.; Barcikowski, S. Optimizing in Vitro Impedance and Physico-Chemical Properties of Neural Electrodes by Electrophoretic Deposition of Pt Nanoparticles. *Chemphyschem Eur. J. Chem. Phys. Phys. Chem.* **2017**, *18*, 1108–1117. [[CrossRef](#)] [[PubMed](#)]
17. Abdulkaki, A.; Doll, T.; Helgers, S.; Heissler, H.E.; Voges, J.; Krauss, J.K.; Schwabe, K.; Alam, M. Subthalamic Nucleus Deep Brain Stimulation Restores Motor and Sensorimotor Cortical Neuronal Oscillatory Activity in the Free-Moving 6-Hydroxydopamine Lesion Rat Parkinson Model. *Neuromodulation* **2023**, *in press*. [[CrossRef](#)] [[PubMed](#)]
18. Paxinos, G.; Watson, C. *The Rat Brain in Stereotaxic Coordinates*, 6th ed.; Academic Press: Cambridge, MA, USA, 2006; ISBN 9780080475158.
19. Nichols, W.T.; Sasaki, T.; Koshizaki, N. Laser Ablation of a Platinum Target in Water. I. Ablation Mechanisms. *J. Appl. Phys.* **2006**, *100*, 114911. [[CrossRef](#)]
20. Streubel, R.; Bendt, G.; Gökce, B. Pilot-Scale Synthesis of Metal Nanoparticles by High-Speed Pulsed Laser Ablation in Liquids. *Nanotechnology* **2016**, *27*, 205602. [[CrossRef](#)]
21. Streich, C.; Koenen, S.; Lelle, M.; Peneva, K. Influence of Ligands in Metal Nanoparticle Electrophoresis for the Fabrication of Biofunctional Coatings. *Appl. Surf. Sci.* **2015**, *348*, 92–99. [[CrossRef](#)]
22. Koenen, S.; Streubel, R.; Jakobi, J.; Schwabe, K.; Krauss, J.K.; Barcikowski, S. Continuous Electrophoretic Deposition and Electrophoretic Mobility of Ligand-Free, Metal Nanoparticles in Liquid Flow. *J. Electrochem. Soc.* **2015**, *162*, D174. [[CrossRef](#)]
23. Abidian, M.R.; Corey, J.M.; Kipke, D.R.; Martin, D.C. Conducting-Polymer Nanotubes Improve Electrical Properties, Mechanical Adhesion, Neural Attachment, and Neurite Outgrowth of Neural Electrodes. *Small* **2010**, *6*, 421–429. [[CrossRef](#)] [[PubMed](#)]
24. Fattahi, P.; Yang, G.; Kim, G.; Abidian, M.R. A Review of Organic and Inorganic Biomaterials for Neural Interfaces. *Adv. Mater.* **2014**, *26*, 1846–1885. [[CrossRef](#)] [[PubMed](#)]
25. Ludwig, K.A.; Langhals, N.B.; Joseph, M.D.; Richardson-Burns, S.M.; Hendricks, J.L.; Kipke, D.R. Poly(3,4-Ethylenedioxythiophene) (PEDOT) Polymer Coatings Facilitate Smaller Neural Recording Electrodes. *J. Neural Eng.* **2011**, *8*, 014001. [[CrossRef](#)]
26. Butson, C.R.; Moks, C.B.; McIntyre, C.C. Sources and Effects of Electrode Impedance during Deep Brain Stimulation. *Clin. Neurophysiol. Off. J. Int. Fed. Clin. Neurophysiol.* **2006**, *117*, 447–454. [[CrossRef](#)]
27. Leach, J.B.; Achyuta, A.K.H.; Murthy, S.K. Bridging the Divide between Neuroprosthetic Design, Tissue Engineering and Neurobiology. *Front. Neuroeng.* **2010**, *2*, 18. [[CrossRef](#)]
28. Liu, X.; McCreery, D.B.; Carter, R.R.; Bullara, L.A.; Yuen, T.G.; Agnew, W.F. Stability of the Interface between Neural Tissue and Chronically Implanted Intracortical Microelectrodes. *IEEE Trans. Rehabil. Eng.* **1999**, *7*, 315–326. [[CrossRef](#)]

29. Nicolelis, M.A.L.; Dimitrov, D.; Carmena, J.M.; Crist, R.; Lehew, G.; Kralik, J.D.; Wise, S.P. Chronic, Multisite, Multielectrode Recordings in Macaque Monkeys. *Proc. Natl. Acad. Sci. USA* **2003**, *100*, 11041–11046. [[CrossRef](#)] [[PubMed](#)]
30. Polikov, V.S.; Tresco, P.A.; Reichert, W.M. Response of Brain Tissue to Chronically Implanted Neural Electrodes. *J. Neurosci. Methods* **2005**, *148*, 1–18. [[CrossRef](#)]
31. Kronenbueger, M.; Nolte, K.W.; Coenen, V.A.; Burgunder, J.-M.; Krauss, J.K.; Weis, J. Brain Alterations with Deep Brain Stimulation: New Insight from a Neuropathological Case Series. *Mov. Disord.* **2015**, *30*, 1125–1130. [[CrossRef](#)]
32. Wei, X.F.; Grill, W.M. Impedance Characteristics of Deep Brain Stimulation Electrodes in Vitro and in Vivo. *J. Neural Eng.* **2009**, *6*, 046008. [[CrossRef](#)]
33. Satzer, D.; Yu, H.; Wells, M.; Padmanaban, M.; Burns, M.R.; Warnke, P.C.; Xie, T. Deep Brain Stimulation Impedance Decreases Over Time Even When Stimulation Settings Are Held Constant. *Front. Hum. Neurosci.* **2020**, *14*, 584005. [[CrossRef](#)]
34. Wong, J.; Gunduz, A.; Shute, J.; Eisinger, R.; Cernera, S.; David Ho, K.W.; Martinez-Ramirez, D.; Almeida, L.; Wilson, C.A.; Okun, M.S.; et al. Longitudinal Follow-up of Impedance Drift in Deep Brain Stimulation Cases. *Tremor Other Hyperkinetic Mov.* **2018**, *8*, 542. [[CrossRef](#)]
35. Bärsch, N.; Jakobi, J.; Weiler, S.; Barcikowski, S. Pure Colloidal Metal and Ceramic Nanoparticles from High-Power Picosecond Laser Ablation in Water and Acetone. *Nanotechnology* **2009**, *20*, 445603. [[CrossRef](#)] [[PubMed](#)]
36. Dahl, J.A.; Maddux, B.L.S.; Hutchison, J.E. Toward Greener Nanosynthesis. *Chem. Rev.* **2007**, *107*, 2228–2269. [[CrossRef](#)] [[PubMed](#)]
37. Heinemann, A.; Koenen, S.; Schwabe, K.; Rehbock, C.; Barcikowski, S. How Electrophoretic Deposition with Ligand-Free Platinum Nanoparticles Affects Contact Angle. *Key Eng. Mater.* **2015**, *654*, 218–223. [[CrossRef](#)]
38. Jakobi, J.; Menéndez-Manjón, A.; Chakravadhanula, V.S.K.; Kienle, L.; Wagener, P.; Barcikowski, S. Stoichiometry of Alloy Nanoparticles from Laser Ablation of PtIr in Acetone and Their Electrophoretic Deposition on PtIr Electrodes. *Nanotechnology* **2011**, *22*, 145601. [[CrossRef](#)]
39. Ramesh, V.; Giera, B.; Karnes, J.J.; Stratmann, N.; Schaufler, V.; Li, Y.; Rehbock, C.; Barcikowski, S. Electrophoretic Deposition of Platinum Nanoparticles Using Ethanol-Water Mixtures Significantly Reduces Neural Electrode Impedance. *J. Electrochem. Soc.* **2022**, *169*, 022504. [[CrossRef](#)]
40. Akhtar, M.A.; Hadzhieva, Z.; Dlouhý, I.; Boccaccini, A.R. Electrophoretic Deposition and Characterization of Functional Coatings Based on an Antibacterial Gallium (III)-Chitosan Complex. *Coatings* **2020**, *10*, 483. [[CrossRef](#)]
41. Besra, L.; Liu, M. A Review on Fundamentals and Applications of Electrophoretic Deposition (EPD). *Prog. Mater. Sci.* **2007**, *52*, 1–61. [[CrossRef](#)]
42. Evers, J.; Sridhar, K.; Liegey, J.; Brady, J.; Jahns, H.; Lowery, M. Stimulation-Induced Changes at the Electrode-Tissue Interface and Their Influence on Deep Brain Stimulation. *J. Neural Eng.* **2022**, *19*, 046004. [[CrossRef](#)]
43. Maddah, M.; Unsworth, C.P.; Gouws, G.J.; Plank, N.O.V. Synthesis of Encapsulated ZnO Nanowires Provide Low Impedance Alternatives for Microelectrodes. *PLoS ONE* **2022**, *17*, e0270164. [[CrossRef](#)] [[PubMed](#)]
44. Chen, K.J.; Oswald, J.; Krüger, T. Electrophoretic Deposition of Dielectric Film on Stimulation Electrodes for the Use in Intraoperative Neuromonitoring. *Curr. Dir. Biomed. Eng.* **2018**, *4*, 521–524. [[CrossRef](#)]
45. Van der Biest, O.O.; Vandeperre, L.J. Electrophoretic Deposition of Materials. *Annu. Rev. Mater. Sci.* **1999**, *29*, 327–352. [[CrossRef](#)]

Disclaimer/Publisher’s Note: The statements, opinions and data contained in all publications are solely those of the individual author(s) and contributor(s) and not of MDPI and/or the editor(s). MDPI and/or the editor(s) disclaim responsibility for any injury to people or property resulting from any ideas, methods, instructions or products referred to in the content.